

Relationship Between X-ray Luminosity and Magnetic Flux of Active Regions and X-ray Bright Points

Kelvin Scheurer^{1,2} and Keiji Yoshimura¹

¹Montana State University ²University Of Wisconsin-La Crosse



Introduction

Studying the relationship between magnetic fields and coronal emission is one way to approach the coronal heating problem. A clear power-law relationship between total unsigned magnetic flux and X-ray spectral luminosity over 12 orders of magnitude was reported in Pevtsov et al. (2003). In a recent study, Yoshimura et al. (2024) identified the cutoff magnetic field strength (B_c) as a key parameter in influencing the power-law relationship. While Yoshimura et al. (2024) focused only on full sun data, we will expand the dataset to include XBPs and ARs utilizing data from Hinode/XRT and SDO/HMI. Using this data will allow for a more detailed analysis on the power-law relationship and the parameters dependency between XBPs and ARs.

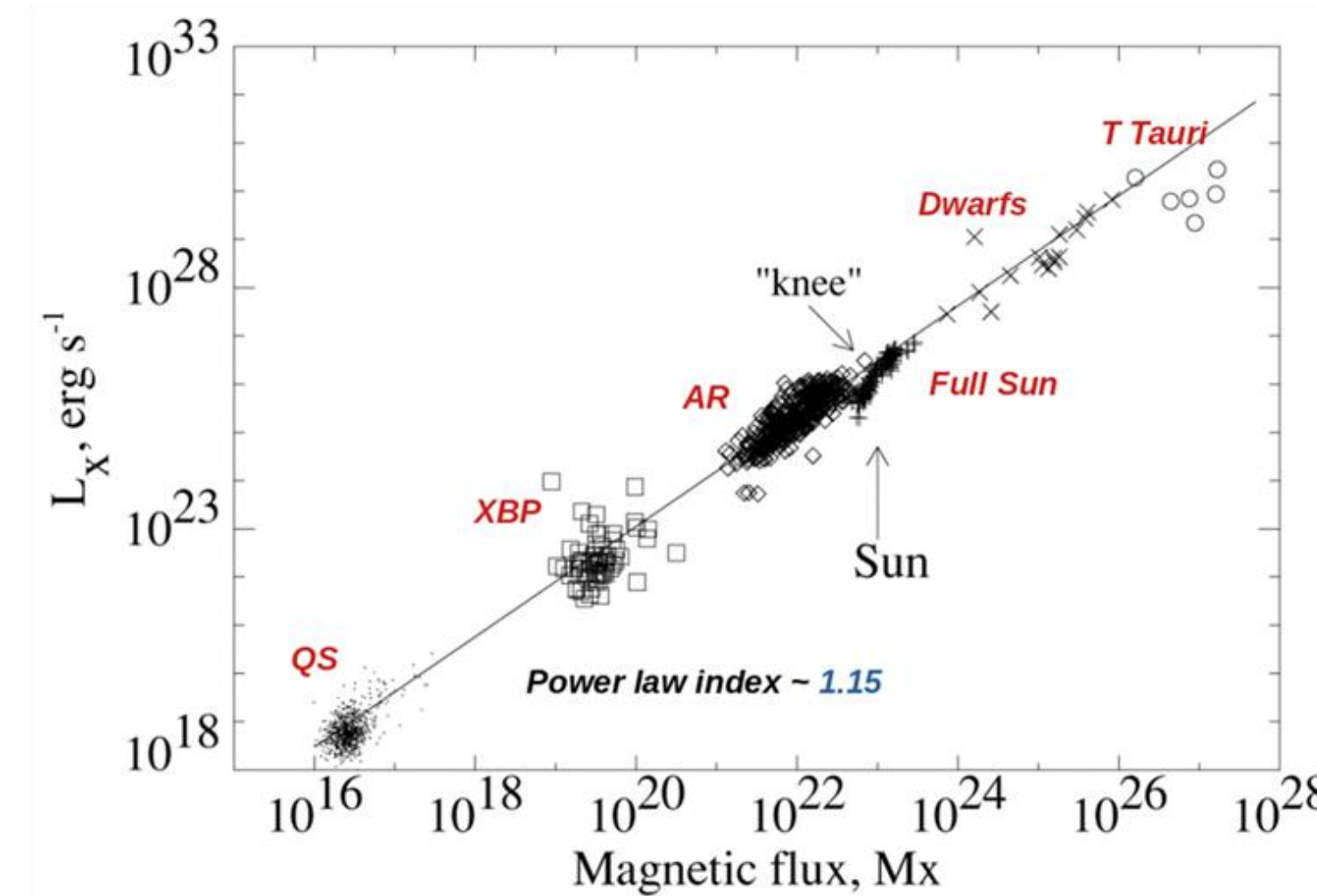


Figure 1: From Pevtsov et al. 2003.

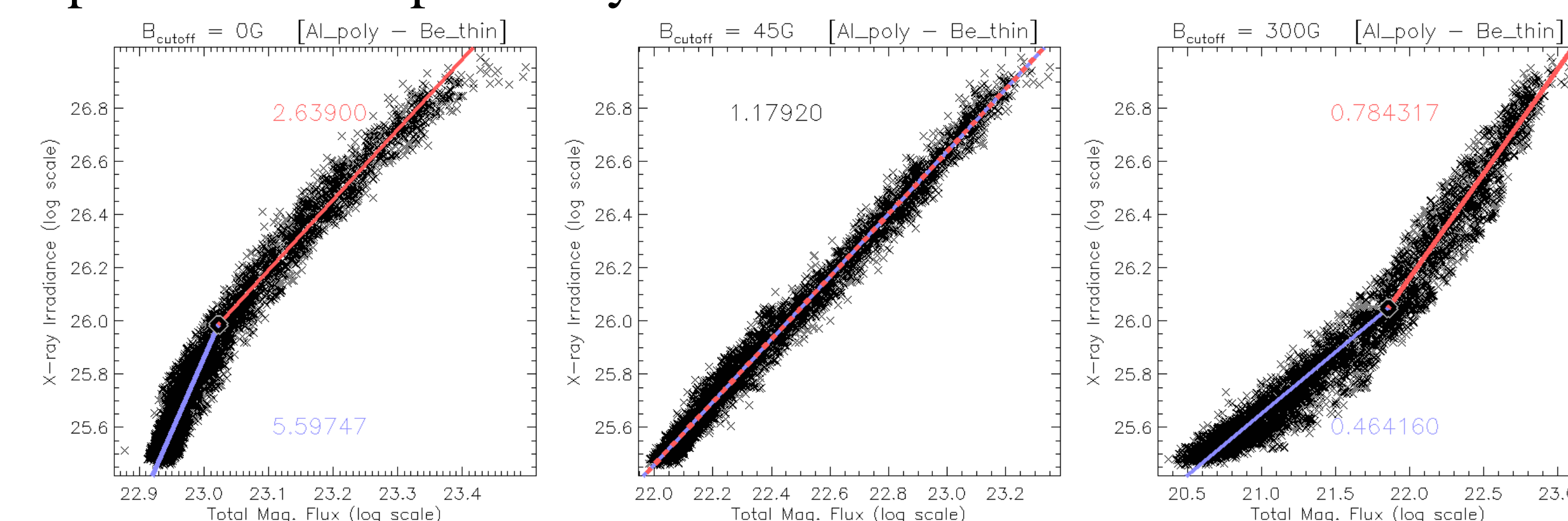


Figure 2: From Yoshimura et al., 2024. Shows different B_c cause different distribution.

Methods

Over a span of 13 years, composite images (Takeda et al., 2016) were compiled using data from Hinode/XRT, using five different filter wheels (FW). We focused on selecting XBPs and ARs using two different thresholds of X-ray intensity in the Thin_be filter. Once the regions were identified, we proceeded to calculate the temperature (T_e) and emission measure (EM) using the filter ratio method. Using derived T_e and EM we synthesized the X-ray spectrum. Integrating over the X-ray spectrum allows us to determine the X-ray luminosity. Next, projecting the selected regions from XRT onto HMI data, we calculated the total unsigned magnetic flux.

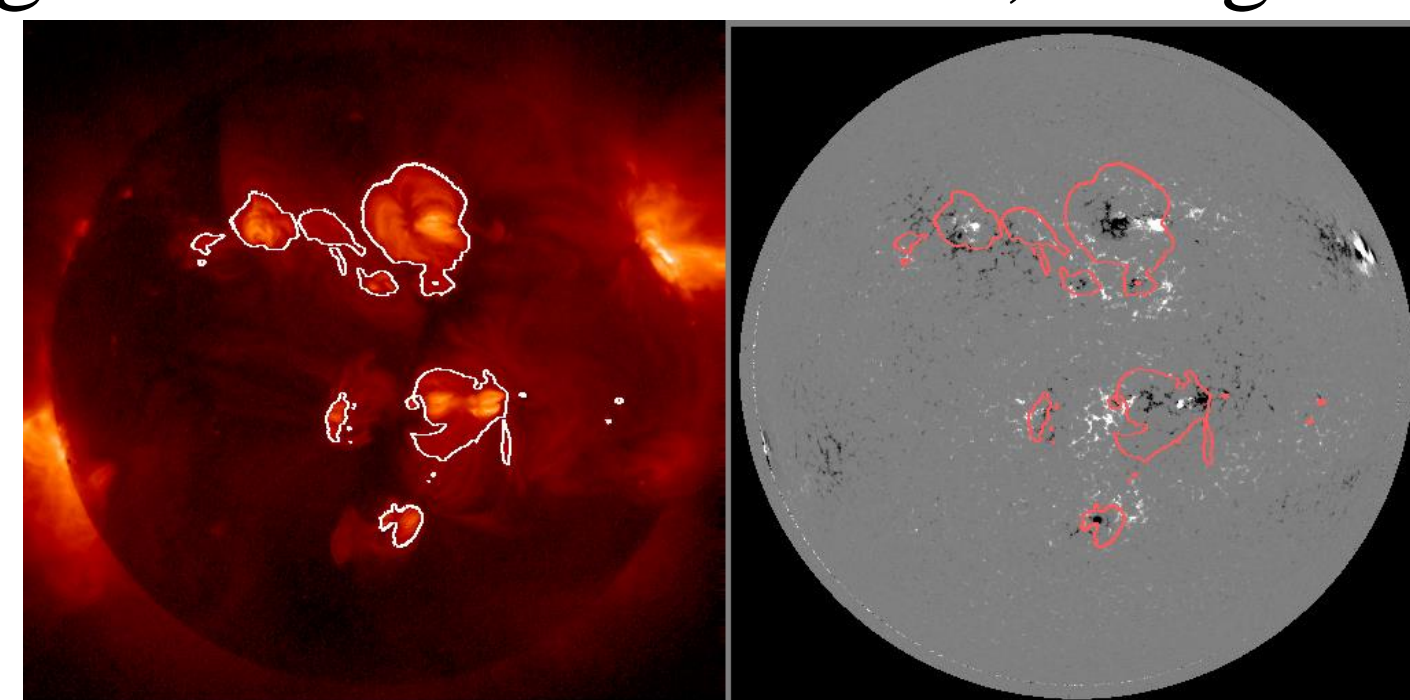


Figure 3: XRT Thin_be image (left) and HMI magnetogram (right) taken on 2024/03/01. The selected areas are shown on the maps with contours.

Results

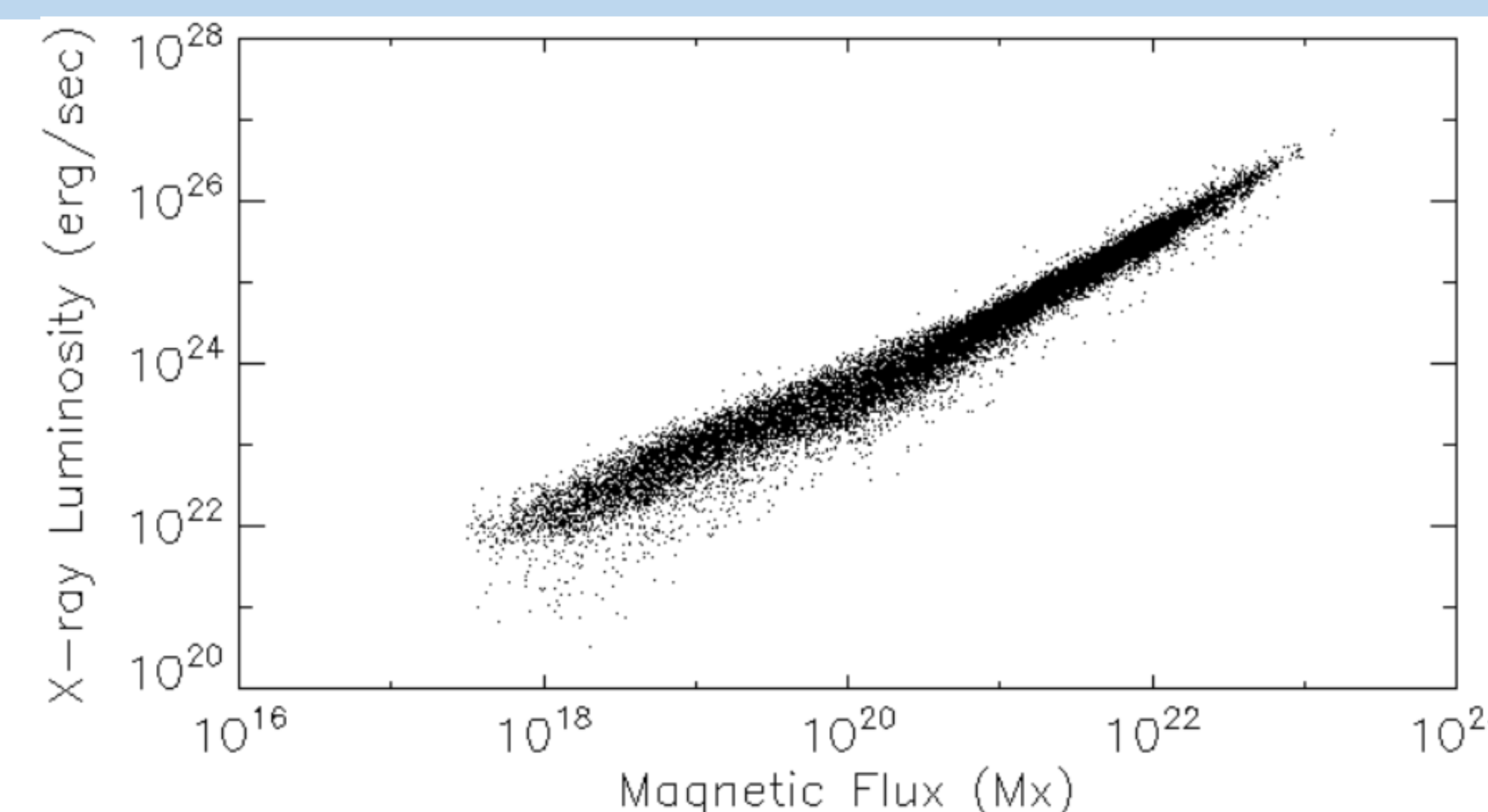


Figure 4: Graph of X-ray luminosity against magnetic flux. X-ray intensity threshold of 40 DN/sec, FW of Al_poly, and a B_c of 0G.

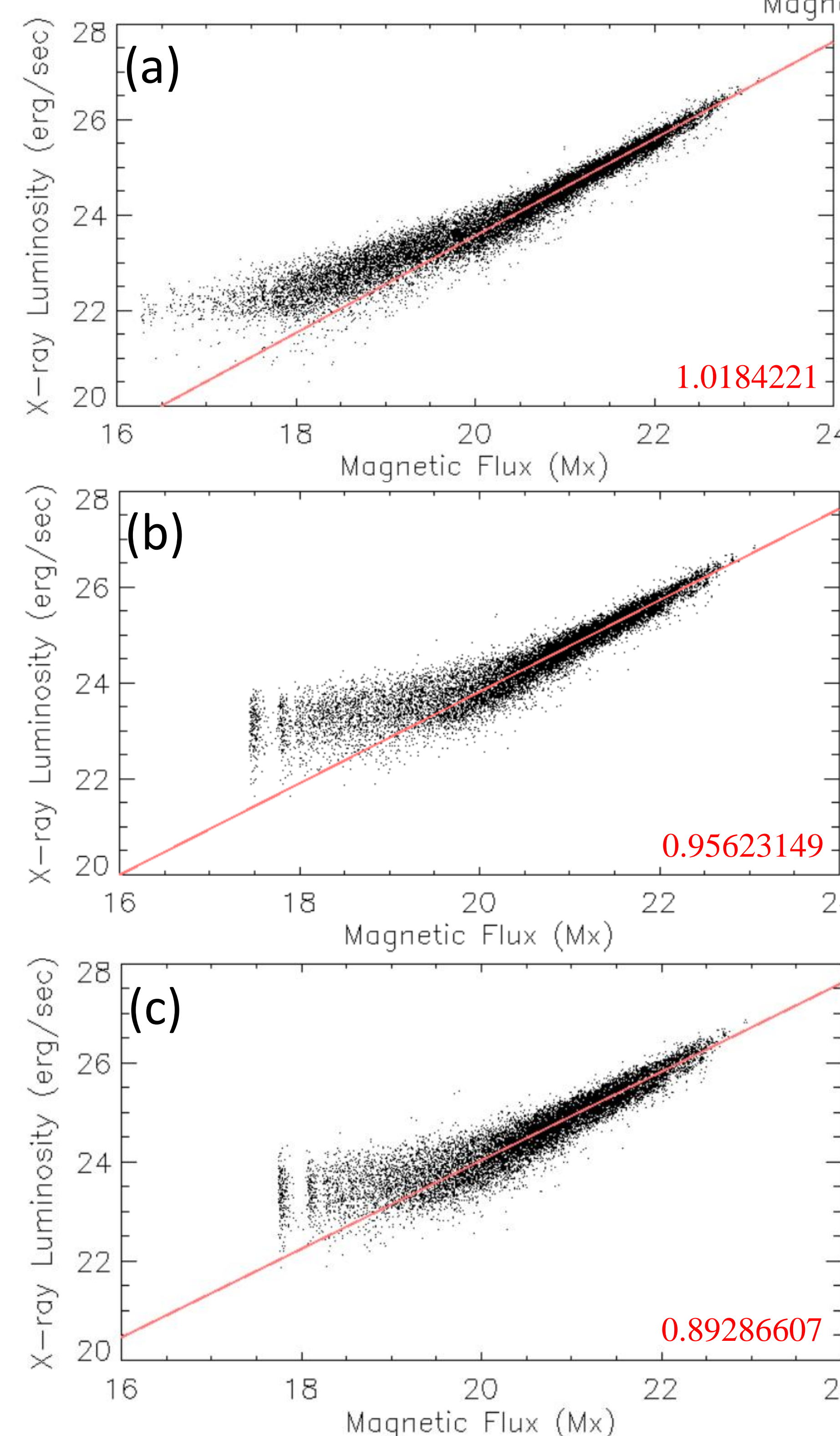


Figure 5: Log-log scale graph showing X-ray luminosity against magnetic flux and the power-law index in red. X-ray intensity threshold of 40 DN/sec, FW of Thin_be and Al_poly, and a B_c of 10 G (a), 150 G (b), and 300 G (c).

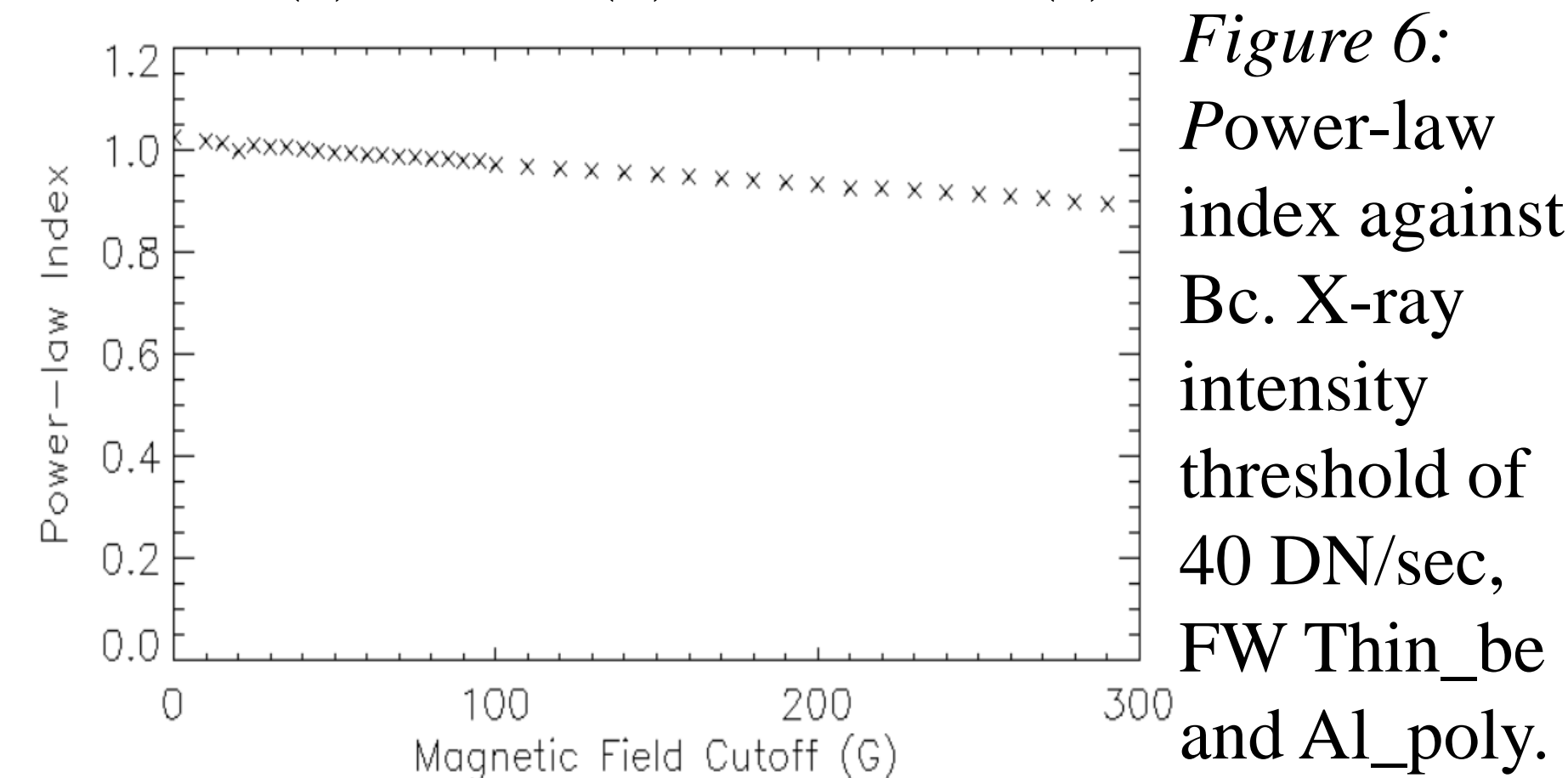


Figure 6: Power-law index against B_c . X-ray intensity threshold of 40 DN/sec, FW Thin_be and Al_poly.

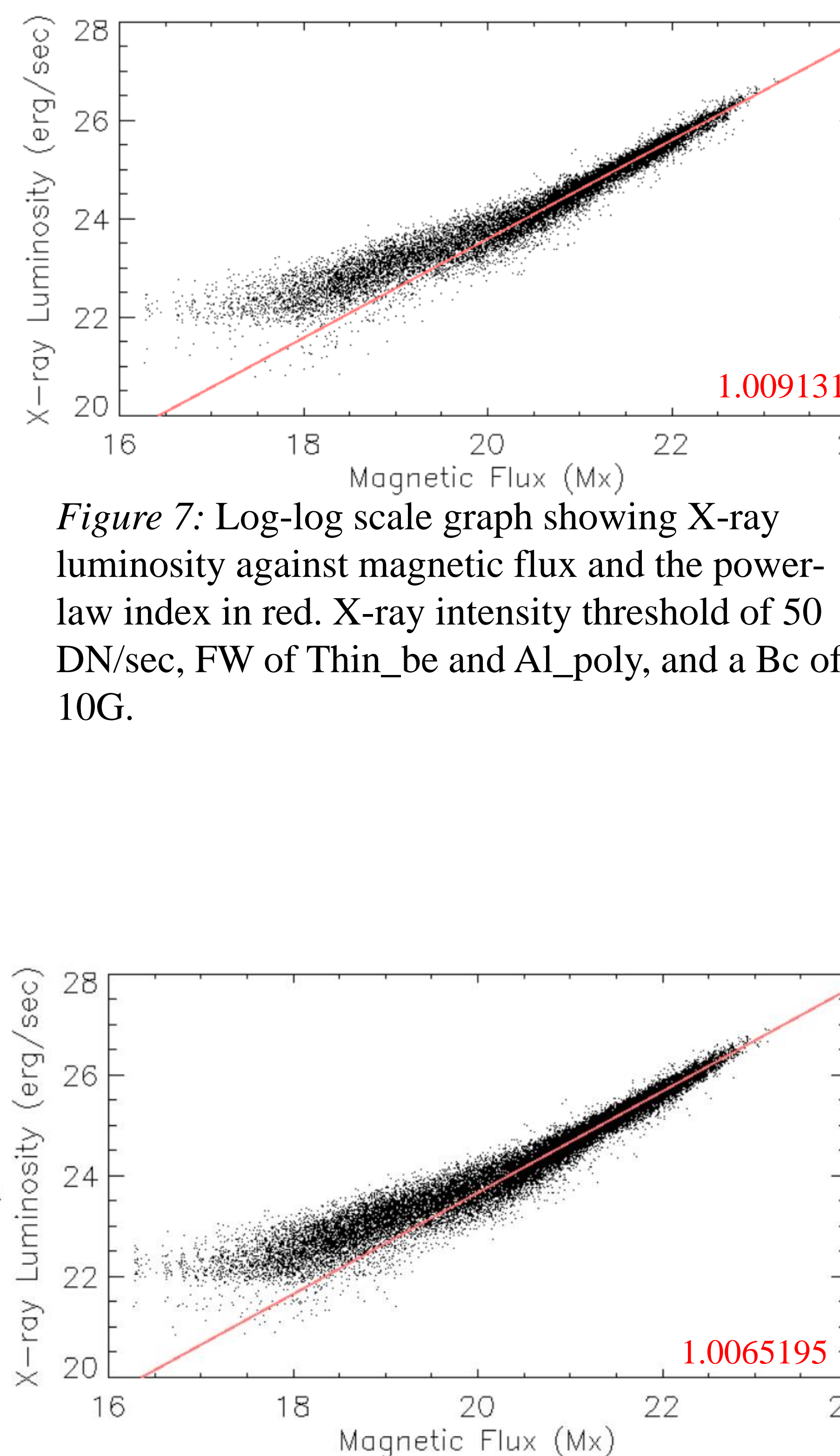


Figure 7: Log-log scale graph showing X-ray luminosity against magnetic flux and the power-law index in red. X-ray intensity threshold of 50 DN/sec, FW of Thin_be and Al_poly, and a B_c of 10G.

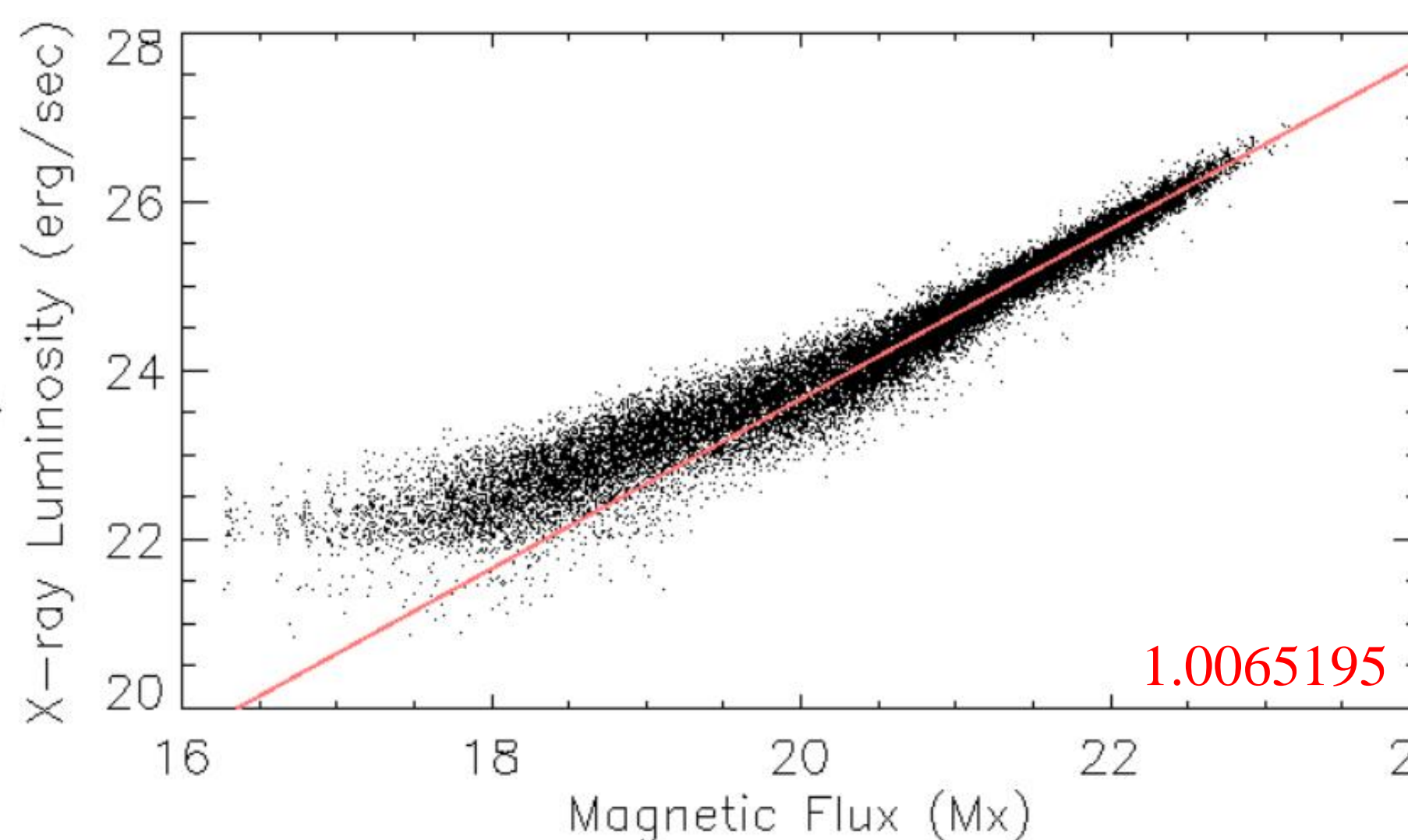


Figure 8: Log-log scale graph showing X-ray luminosity against magnetic flux and the power-law index in red. X-ray intensity threshold of 40 DN/sec, FW of Thin_be and Al_mesh, and a B_c of 10G.

Results

- Figure 4 shows that we have successfully covered 5 orders of magnitude ranging between the lower XBP and upper AR.
- We fitted data points above 10^{21} Mx (red line) to derive power-law index (Figure 5).
- Figure 6 visibly shows the power-law index with increasing B_c . With increasing magnetic field strength follows a slightly decreasing power-law index.
- Changing to the another threshold doesn't show any significant difference of power-law index values (Figure 7).
- Changing to another FW (Thin_be and Al_mesh) doesn't show any significant difference of power-law index values (Figure 8).

Discussion and Future Work

- Data points below 10^{21} Mx shows different trend. This could be caused by a genuine phenomenon in nature or due to data selection bias.
- Comparing results with Yoshimura et al. (2024) the change of the power-law index in our study is smaller.
- Fisher et al. (1998) reported a power-law index of 1.19 while ours remained smaller for all B_c .
- The general trend of the power-law index appears to be decreasing with B_c regardless of the selected FWs and of the two X-ray intensity threshold options.

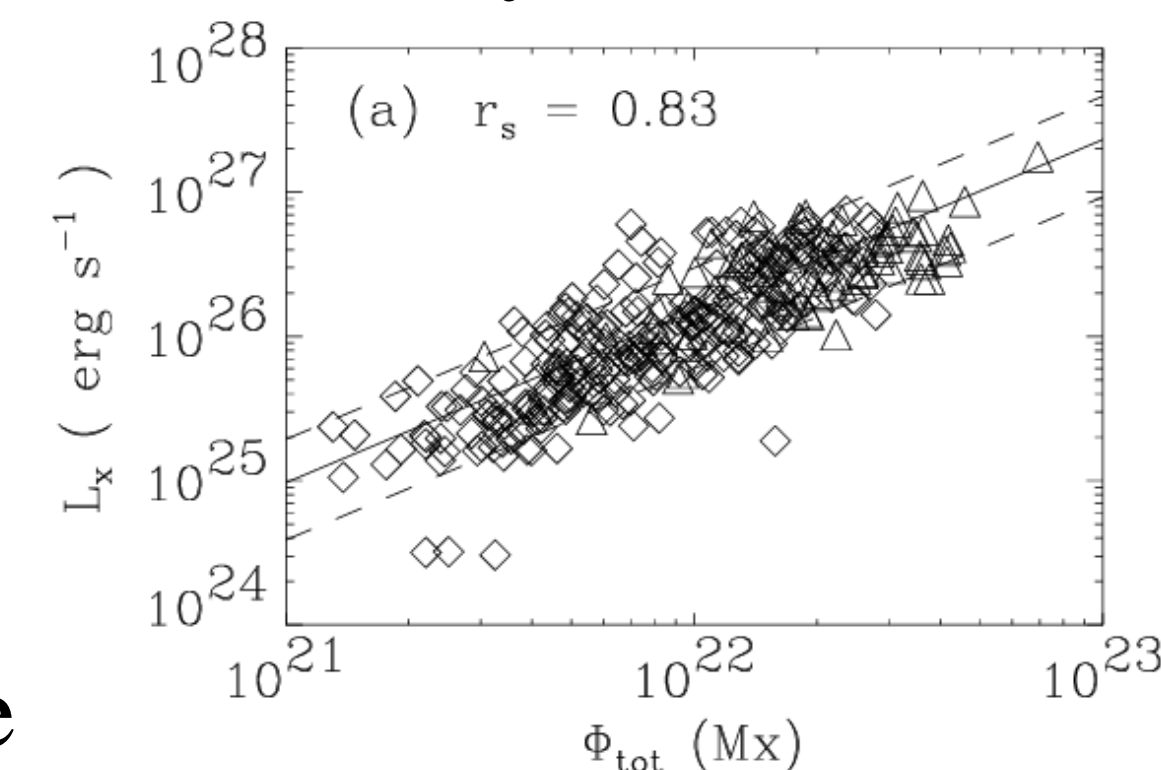


Figure 9: From Fisher et al. 1998. Used Yohkoh/SXT and HSP (Haleakala Stokes Polarimeter) magnetogram data.

Future Work

- Adjust/modify the way to project the selected AR areas to HMI data.
- Look into the cause of the different trend below 10^{21} Mx.

Acknowledgements

This research was funded by NSF award #: 2244344

References

- Fisher et al., 1998, ApJ, 508, 885
 Pevtsov et al., 2003, ApJ, 598, 1387
 Takeda et al., 2016, Sol.Phys., 291, 317
 Yoshimura et al., 2024, TESS 2024 Meeting at Dallas, TX, USA